JCTC Journal of Chemical Theory and Computation

Computation of Accurate Activation Barriers for Methyl-Transfer Reactions of Sulfonium and Ammonium Salts in Aqueous Solution

Hakan Gunaydin,[†] Orlando Acevedo,[‡] William L. Jorgensen,*,[‡] and K. N. Houk*,[†]

Department of Chemistry and Biochemistry, University of California, Los Angeles, California 90095-1569, and Department of Chemistry, Yale University, 225 Prospect Street, New Haven, Connecticut 06520-8107

Abstract: The energetics of methyl-transfer reactions from dimethylammonium, tetramethylammonium, and trimethylsulfonium to dimethylamine were computed with density functional theory, MP2, CBS-QB3, and quantum mechanics/molecular mechanics (QM/MM) Monte Carlo methods. At the CBS-QB3 level, the gas-phase activation enthalpies are computed to be 9.9, 15.3, and 7.9 kcal/mol, respectively. MP2/6-31+G(d,p) activation enthalpies are in best agreement with the CBS-QB3 results. The effects of aqueous solvation on these reactions were studied with polarizable continuum model, generalized Born/surface area (GB/SA), and QM/MM Monte Carlo simulations utilizing free-energy perturbation theory in which the PDDG/PM3 semiempirical Hamiltonian for the QM and explicit TIP4P water molecules in the MM region were used. In the aqueous phase, all of these reactions proceed more slowly when compared to the gas phase, since the charged reactants are stabilized more than the transition structure geometries with delocalized positive charges. In order to obtain the aqueous-phase activation free energies, the gas-phase activation free energies were corrected with the solvation free energies obtained from single-point conductor-like polarizable continuum model and GB/SA calculations for the stationary points along the reaction coordinate.

Introduction

The transfer of methyl groups is a widely observed process in biological pathways; methyl groups are routinely transferred to reaction intermediates during the synthesis of a variety of compounds such as lignin, phenylpropene, some alkaloids, and phospholipids.[1−4] Enzymes that catalyze methyl-transfer reactions generally utilize compounds with active methyl substituents such as S-adenosyl-L-methionine (SAM).[1−7] The cofactor SAM is involved in several transmethylation reactions, such as the synthesis of neurotransmitters in the brain.[5,6] Catechol *O*-methyl-transferase utilizes SAM as the methyl source for the methylation of cytosine,

adenine, and catechol.[7,8] Modification of adenine within DNA through the transfer of a methyl group is a common defense mechanism in biological organisms that enables them to distinguish host DNA from viral DNA.[8] In addition, three different types of methyl-transfer enzymes are known to utilize SAM to transfer methyl groups to DNA.[9]

In order to understand the magnitude of the enzymatic acceleration of methyl-transfer reactions, it is important to know the rate of methyl-transfer reactions in water in the absence of protein (background reaction). These uncatalyzed rate constants (k_{noncat}) are used to calculate the rate enhancements (k_{cat}/k_{noncat}) and proficiencies [$(k_{cat}/K_M)/k_{noncat}$] of the enzymes.[10] For slow reactions, Wolfenden and Callahan have estimated uncatalyzed rates by measuring the rate constants at elevated temperatures and extrapolating them to room temperature.[10] An alternative approach is to compute the activation energies of these uncatalyzed reactions. In order

* Corresponding authors. E-mail: houk@chem.ucla.edu (K.N.H.), william.jorgensen@yale.edu (W.L.J.).
† University of California, Los Angeles.
‡ Yale University.

Scheme 1. Methyl-Transfer Reactions in Aqueous Phase Studied by Wolfenden
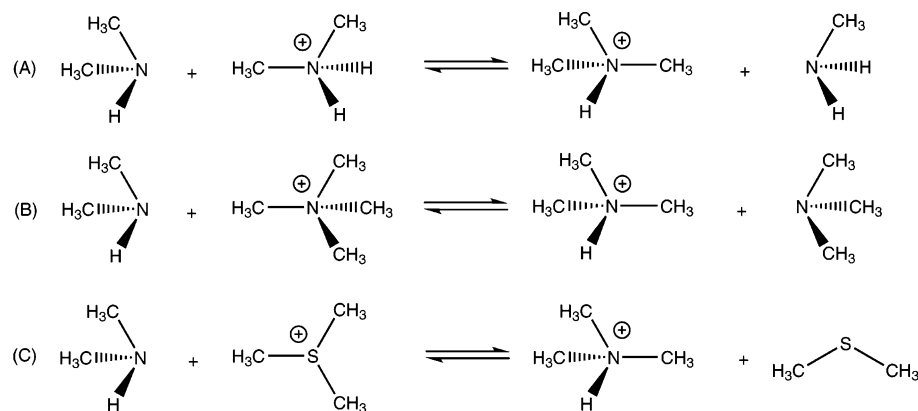
to estimate the aqueous-phase rate constants with good accuracy, reliable solvation energies need to be generated. This is a very challenging problem that has attracted much attention. Warshel and Weiss have approached this problem by developing the empirical valence bond (EVB) method to generate an approximate potential energy surface for reactions in solution.[11a] EVB was used to compute the activation energies for a variety of background reactions with reasonable accuracy; these were subsequently compared to enzymatic reactions.[11] Warshel demonstrated that enzymes provide a more efficient charge stabilization environment for the transition structures (TSs) by anchoring side-chain and backbone dipoles in appropriate orientations.[11b] The free-energy profile for the hydrolysis of the phosphate ester in solution was also studied using Langevin dipoles and polarized continuum methods.[11c] Detailed investigation for the general base-catalyzed methanolysis of formamide was also carried out, and it was found that the gas-phase reaction

paths did not provide an adequate model for the reactions in solution, emphasizing the need for accurate solvation methods.[11d]

Wolfenden and Callahan measured the activation parameters of the three methyl-transfer reactions that are shown in Scheme 1.[10] The rate of the uncatalyzed methyl-transfer reaction from trimethylsulfonium to dimethyamine in the aqueous phase was used to obtain the catalytic rate enhancement of the enzyme histamine N-methyl-transferase that catalyzes the metabolism of histamine and is responsible for the termination of the neurotransmitter action of histamine in the brain.[6,10] It was found that this enzyme enhances the rate of the methyl-transfer reaction by 5×10^{13}.[10] The rate enhancement of catechol *O*-methyltransferase, which catalyzes the transfer of the methyl group from SAM to an oxygen nucleophile, is reported to be on the order of 10^{17} by using the same uncatalyzed rate constant for this enzyme.[10]
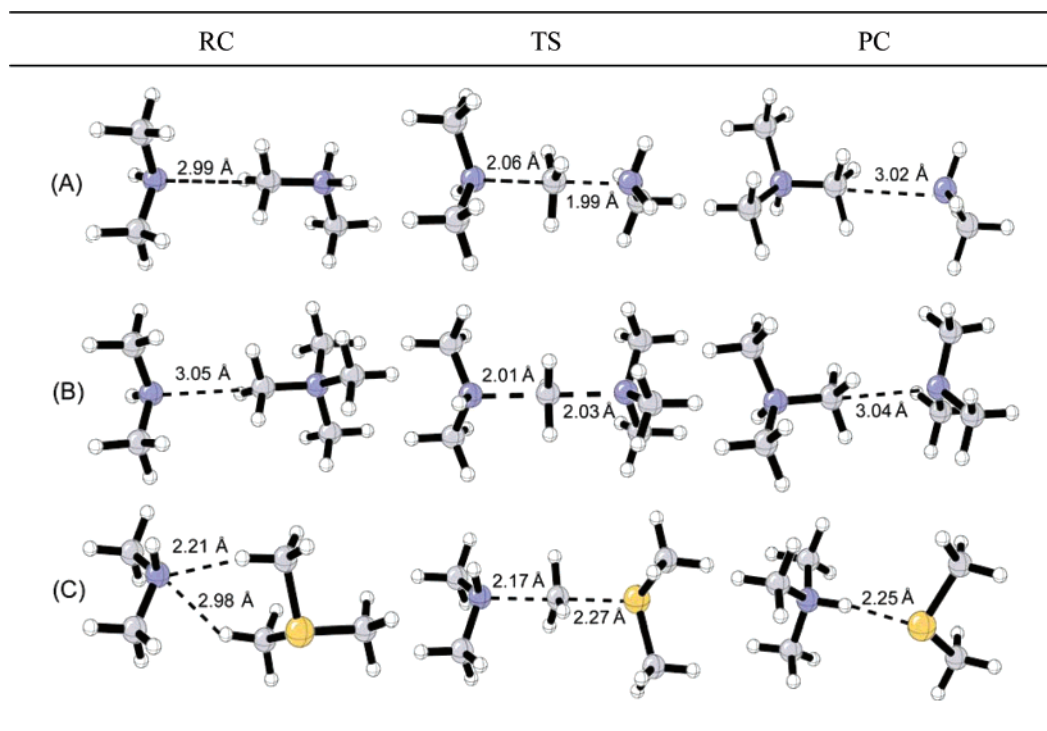

Figure 1. Geometries of stationary points for reactions A, B, and C located at the B3LYP/6-31+G(d,p) level. RC: reactive complex, TS: transition state, PC: product complex. Full geometrical parameters are given in the Supporting Information.

The factors controlling the catalytic efficiency of catechol *O*-methyltransferase have been investigated theoretically.[12] Roca et al. calculated the activation free energy of methyl-transfer reactions from trimethylsulfonium to the catecholate ion in water and from SAM to the catecholate ion in water and in an enzyme environment by making use of the quantum mechanics/molecular mechanics (QM/MM) methodology.[12a] The QM/MM computed activation free energy for the aqueous methyl-transfer reaction (26.9 kcal/mol) was found to be in reasonable agreement with the experimental estimate (30.8 kcal/mol) of this methyl-transfer reaction. The reasons behind the efficiency of the enzymatic reaction over the aqueous-phase reaction have been discussed in detail.[12a] In addition, the same catalytic and aqueous-phase reactions have been studied by using quantum mechanics/free-energy simulations (QM−FE) by Kuhn and Kollman.[12b] The QM−FE barriers for the enzymatic and aqueous-phase methyl-transfer reactions are reported to be 24.5 and 29.5 kcal/mol, respectively. Bruice and Zheng have calculated the gas-phase and condensed-phase activation energies for trimethylsulfonium to the catecholate ion by using quantum mechanics.[12c] On the basis of molecular dynamics simulations, it has been shown that the enzyme active site does not change significantly upon binding to either reactants or the transition structure for this methyl-transfer reaction.[12d] Bruice and co-workers have also shown that SAM and catecholate ions spend significant amounts of time in the "near attack conformer" (NAC) and came to the conclusion that the basis of the catalytic power of the catechol *O*-methyl-transferase arises from populating the NACs.[12d,e]

Transfer of a methyl group from trimethylsulfonium to pyridine has been computed previously with the B3LYP/6-31+G(d) level in the gas phase.[13] Effects of solvation on the activation barrier of this reaction with different solvents were investigated. Theoretical calculations revealed that, when the gas-phase density functional theory (DFT) activation free energies were corrected with QM/MM/Monte Carlo (MC) solvation corrections, the computed (25.9 kcal/mol) and experimental (29.6 kcal/mol) activation free energies were in good agreement.[13] In addition, the steric effects of various S_N2 reactions involving chloride and five different chlorocarbons have been computed in the gas phase with CBS-QB3 and PDDG/PM3 methods.[14] The transition-state carbon−chlorine distances computed with CBS-QB3 and PDDG/PM3 were found to be essentially the same in both methods.[14] Solvation corrections for these reactions were calculated using QM/MM/MC simulations as well as the conductor-like polarizable continuum model (CPCM) method, and both methods gave similar condensed-phase activation enthalpies.[14]

The aim of the research described in this paper was to test various quantum mechanical and solvation methods for simple methyl-transfer reactions to determine the appropriate level of theory necessary to reproduce the kinetics of aqueous-phase reactions with high accuracy. The gas-phase reaction mechanisms were computed with DFT, Møller−Plesset perturbation theory, and CBS-QB3 methods. Solvation corrections were obtained with the CPCM, generalized Born/surface area (GB/SA), and free-energy QM/MM/MC
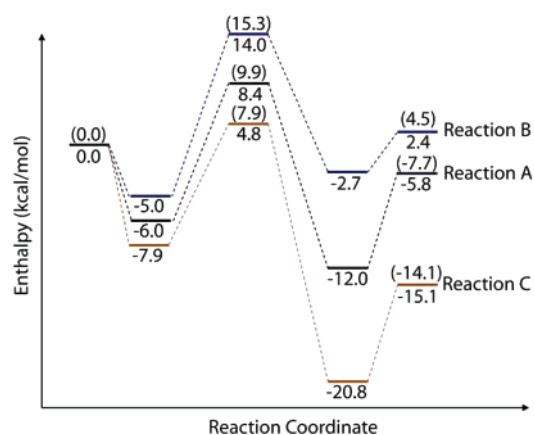
Figure 2. Enthalpies (kcal/mol) calculated with B3LYP/6-31+G(d,p) for the gas phase. CBS-QB3 values for the reactants, transition states, and products are given in parentheses.

Table 1. Activation Enthalpies of Reactions A, B, and C (kcal/mol)

method	reaction A	reaction B	reaction C
B3LYP/6-31G(d)	6.0	11.5	2.2
B3LYP/6-31G(d,p)	6.0	11.7	2.4
B3LYP/6-31+G(d,p)	8.4	14.0	4.8
MPW1K/6-31+G(d,p)	12.4	17.9	9.0
MP2/6-31G(d)	8.7	13.9	5.9
MP2/6-31+G(d,p)	9.8	14.7	7.0
CBS-QB3	9.9	15.3	7.9

Table 2. Activation Free Energies of Reactions A, B, and C (kcal/mol)

method	reaction A	reaction B	reaction C
B3LYP/6-31+G(d,p)	17.9	24.2	13.6
MP2/6-31+G(d,p)	19.9	25.3	16.4
CBS-QB3	19.4	24.8	18.0

simulations using the PDDG/PM3 semiempirical Hamiltonian for the solute and TIP4P water molecules for the solvent.

Methodology

The gas-phase energetics were computed with DFT,[15,16] MP2,[17] and CBS-QB3[18] levels of theory by using Gaussian 98[19] and Gaussian 03.[20] For DFT calculations, the B3LYP[21,22] functional with 6-31G(d), 6-31G(d,p), and 6-31+G(d,p) basis sets and the MPW1K[23] functional with the 6-31+G(d,p) basis set were used. For MP2 calculations, 6-31G(d) and 6-31+G-(d,p) basis sets were used. The accuracies of these methods and basis sets were tested against the more accurate CBS-QB3 activation energies.

Solvation effects for these reactions were studied by using the CPCM[24] method and GB/SA[25−27] as implemented in the BOSS program.[28] Single-point CPCM and GB/SA calculations were utilized for all of the stationary points located in the gas phase in order to obtain the solvation free energies for the reactants, products, and transition structures. The gas-phase activation free energies were corrected with these solvation corrections to estimate the activation free energies

Computation of Accurate Activation Barriers

J. Chem. Theory Comput., Vol. 3, No. 3, 2007 **1031**

Table 3. Enthalpies of the Reactant Complexes (RC), Transition Structures (TS), Product Complexes (PC), and Products (P) Relative to the Reactants (R) at Infinite Separation (kcal/mol) [BS1:6-31G(d), BS2:6-31+G(d,p)]

	reaction A				reaction B				reaction C			
	B3LYP		MP2		B3LYP		MP2		B3LYP		MP2	
	BS1	BS2	BS2	CBS-QB3	BS1	BS2	BS2	CBS-QB3	BS1	BS2	BS2	CBS-QB3
R	0	0	0	0	0	0	0	0	0	0	0	0
RC	−7.4	−6.0	−8.1		−6.3	−5.0	−2.1[a]		−9.8	−7.9	−13.3	
TS	6.0	8.4	9.8	9.9	11.5	14.0	14.7	15.3	2.2	4.8	7.0	7.9
PC	−12.5	−12.0	−15.5		−4.7	−2.7	2.2[a]		−31.5	−20.8	−33.0	
P	−4.8	−5.8	−7.8	−7.7	1.7	2.4	4.4	4.5	−17.7	−15.1	−17.3	−14.1

[a] Thermal corrections are obtained from HF calculations with the same basis set.

in the aqueous phase. Benchmarking studies showed that, when CM1A[29,30] charges are used in conjunction with GB/SA solvation corrections, experimental hydration free energies can be reproduced with a high accuracy.[25−27] The GB/SA solvation free energies for the methyl-transfer reactions studied here were computed by using the methodology described by refs 25−27.

QM/MM/MC simulations from BOSS were used to obtain the hydration free energies with explicit solute−solvent interactions by making use of statistical averaging of the possible configurations. The QM/MM method has been established as a good technique for studying the chemical reactions in both solution and enzyme environments.[31] Several QM/MM methods have been utilized, and these methods differ in their treatment of the quantum mechanical and/or molecular mechanics regions.[31] An overview of the applications of the QM/MM method for studying enzyme reactivity has been published by Gogonea.[31a] In order to determine the effect of solvation on the reaction coordinate, free-energy perturbation (FEP) calculations were carried out in the NPT ensemble. In these FEP calculations, the solutes were treated in the QM region and water molecules were described in the MM region. The configurational space was explored using the Metropolis Monte Carlo algorithm. This method has been shown to give excellent results for S_N2 reactions,[14] nucleophilic aromatic substitution reactions,[32a] Kemp decarboxylations,[32b,c] and Cope elimination[32d] reactions. In these FEP simulations, the reaction coordinates were explored with increments of 0.01 Å by the sampling of all other degrees of freedom from separated reactants to the products through transition states. Since this procedure requires ca. 15 million single-point QM calculations per system, the use of the fast semiempirical PDDG/PM3[33] QM method was necessary. The solvent water molecules were represented with the TIP4P water model.[34] For electrostatic contributions to the solute−solvent energy, unscaled CM1 charges were calculated for the solute with the PDDG/PM3 Hamiltonian. For each heavy atom of the solutes, one water molecule was extracted from the pre-equilibrated solvent box of 750 water molecules to make space for the solutes. Simulations were run at 25 °C and 1 atm. In each simulation, equilibration of 2.5 M configurations was followed by averaging of 5 M configurations. In this method, the interaction between the QM region and MM region is treated through nonbonded electrostatic interactions and Lennard-Jones parameters. Solute−solvent and solvent−solvent intermolecular cutoff distances of 10 Å were applied on the

Table 4. Solvation Free Energies ($\Delta G_{Solvation}$; kcal/mol) Computed with Single-Point CPCM Calculations at the B3LYP/6-31G(d) Level[a]

	$\Delta G_{Solvation}$		
	reaction A	reaction B	reaction C
R1	−4.0	−4.0	−4.0
R2	−65.4	−51.7	−42.1
RC	−59.5	−46.9	−37.6
TS	−52.5	−47.5	−40.3
PC	−54.2	−52.5	−42.8
P	−64.4	−62.4	−61.1

[a] R1 represents dimethyl amine, and R2 represents the second reactant in each reaction.

basis of center of mass separations. A feathering of the intermolecular interactions within 0.5 Å of the cutoff was applied. This methodology gives accurate results for charged and neutral species.[14,32]

Results and Discussion

Gas-Phase Calculations. Methyl transfers from charged ammonium or sulfonium compounds to neutral amines proceed via an S_N2 reaction mechanism. The methyl group inverts during the reaction in a backside displacement process. The geometries for the stationary points obtained at this level of theory are given in Figure 1, and the corresponding potential energy surfaces for these S_N2 reactions in the gas phase, computed at the B3LYP/6-31+G-(d,p) level of theory, are shown in Figure 2. In the gas phase, all three reactions proceed through the formation of reactant and product ion−dipole complexes (RC and PC, respectively, in Figure 1) whose energies are lower than the sum of the reactant energies. The geometries for the ion−dipole complexes were located by following the imaginary frequencies of the transition structures along the reaction path toward reactants and products by intrinsic reaction coordinate (IRC) calculations and then optimizing the last IRC geometries. In order to test the accuracy of various types of calculations, enthalpies are computed with different basis sets and functionals at the DFT and MP2 levels, and these enthalpies are compared to the more accurate CBS-QB3 results (Table 1). Diffuse functions are found to be crucial for the accurate description of these methyl-transfer reactions. MP2/6-31+G-(d,p) activation enthalpies for all three reactions agree best with the activation enthalpies obtained at the CBS-QB3 level. B3LYP/6-31+G(d,p) activation barriers are in good agreement with CBS-QB3 activation barriers for the methyl-

Table 5. Aqueous Phase Reaction and Activation Free Energies and Experimental Activation Free Energies (kcal/mol)[a]

| | reaction A | | | | reaction B | | | | reaction C | | | |
	B3LYP 6-31+G(d,p)	MP2 6-31+G(d,p)	CBS-QB3	exp[10]	B3LYP 6-31+G(d,p)	MP2 6-31+G(d,p)	CBS-QB3	exp[10]	B3LYP 6-31+G(d,p)	MP2 6-31+G(d,p)	CBS-QB3	exp[10]
R	0	0	0	0	0	0	0	0	0	0	0	0
RC	10.7	8.1			10.7	18.4[b]			7.9	4.3		
TS	34.8	36.8	36.3	34.4	32.4	33.5	33.0	33.5	19.4	22.2	23.8	28.1
PC	10.1	5.8			9.5	16.8[b]			−8.0	−22.5		
P	−1.1	−3.1	−3.0		−4.6	−2.6	−2.6		−31.1	−32.5	−28.6	

[a] The solvation effects are computed with single-point CPCM calculations at the B3LYP/6-31G(d) level. [b] Thermal corrections are obtained from HF calculations with the same basis set.

Table 6. Activation Free Energies Computed at the B3LYP/6-31+G(d,p) Level with Different Cavity Methods

| | $\Delta G^{\ddagger}_{Sol}$ | | |
	reaction A	reaction B	reaction C
UAHF	34.8	31.5	19.2
UA0	33.7	31.2	21.5
UAKS	34.7	31.5	19.2
UFF	35.3	30.1	25.2
BONDI	40.5	37.8	28.5
PAULING	41.0	38.4	28.7
exp[10]	34.4	33.5	28.1

transfer reactions from ammonium salts but not for the methyl-transfer reaction from trimethyl sulfonium salt. All of the B3LYP/6-31+G(d,p) activation barriers for the methyl-transfer reactions studied here are found to be lower than the CBS-QB3 activation barriers as expected, since the DFT method is known to underestimate the activation barriers for S_N2 reactions.[35] The CBS-QB3 method generates thermodynamic properties with high accuracy for a variety of molecules, and it has been shown that, for S_N2 reactions, the estimated activation enthalpies differ by 0.5 kcal/mol from even higher accuracy methods like W1[36] and W2[37] or other coupled cluster methods.[38] Therefore, CBS-QB3 activation enthalpies are assumed to produce the best gas-phase results for these reactions among the methods applied. MPW1K/6-31+G(d,p) gave the highest estimates of the activation enthalpies for all three reactions among the methods applied (Table 1). The activation free energies for these reactions in the gas phase with B3LYP/6-31+G(d,p), MP2/6-31+G(d,p), and CBS-QB3 methods are given in Table 2. The energies of the all stationary points located with DFT and MP2 levels of theory with 6-31G(d) and 6-31+G-(d,p) basis sets are given in Table 3.

In the gas phase, reaction A is estimated to be exothermic, and reaction B is estimated to be endothermic (Table 3). The only difference between these two reactions is the different

substituents on the methyl-donor compounds (Scheme 1). In reaction A, the methyl donor dimethylammonium has two hydrogens and two methyl groups, whereas in reaction B, the methyl donor tetramethylammonium has four methyl groups. This increases the reaction enthalpy by 12.2 kcal/mol and the activation enthalpy by 5.4 kcal/mol at the CBS-QB3 level. Possible reasons for the changes in the reaction and activation enthalpies for these two reactions are (i) the electron-donating alkyl substituents on the ammonium cation stabilize the reactants more than the neutral products, and therefore, the transition structure for reaction B is higher in energy than the transition structure for reaction A and (ii) the steric effects generated by the methyl groups might raise the activation enthalpy of reaction B more than that of reaction A. Reaction C involves breaking a carbon−sulfur bond and forming a carbon−nitrogen bond. Therefore, the energetics of this reaction are controlled by the relative strengths of the weaker carbon−sulfur bond on the reactants side and stronger carbon−nitrogen bond on the products side, which causes an early transition structure (Figure 1) and low activation barrier for this reaction.

Aqueous-Phase Calculations. Solvation corrections for the reactions were first computed by single-point CPCM calculations at the B3LYP/6-31G(d) level (Table 4). The polar solvent, water, stabilizes reactants and products with localized charges more than the TSs with delocalized positive charges. Therefore, the activation free energies of the reactions are increased substantially by the aqueous solvent. The RCs are found to be higher in energy than the reactants in the aqueous phase for all three reactions (Table 5).

CBS-QB3 computed activation free energies with single-point CPCM solvation corrections are in good agreement with the available experimental data for reactions A and B but deviate by 3.6 kcal/mol for reaction C (Table 5). The average absolute error for the estimation of the activation free energies with the single-point CPCM corrections for the CBS-QB3 optimized geometries with respect to the experi-

Table 7. Aqueous Phase Reaction and Activation Free Energies Computed at the CBS-QB3 and B3LYP/6-31+G(d) Levels and Experimental Activation Free Energies (kcal/mol)[a]

| | reaction A | | | reaction B | | | reaction C | | |
	B3LYP	CBS-QB3	exp	B3LYP	CBS-QB3	exp	B3LYP	CBS-QB3	exp
R	0.0	0.0	0.0	0.0	0.0	0.0	0.0	0.0	0.0
TS	28.4	29.9	34.4	27.7	28.3	33.5	30.1	34.6	28.1
P	−0.2	−2.1		−2.9	−0.9		−3.5	−2.0	

[a] The solvation free energies are computed with single-point GB/SA calculations for CBS-QB3 geometries.

Computation of Accurate Activation Barriers

J. Chem. Theory Comput., Vol. 3, No. 3, 2007 **1033**

Table 8. GB/SA Solvation Free Energies (kcal/mol) for CBS-QB3 Gas-Phase Geometries

	ΔG_{Solv}		
	reaction A	reaction B	reaction C
R1	−3.4	−3.4	−3.4
R2	−63.8	−50.3	−65.3
TS	−56.7	−50.2	−52.1
P	−61.5	−58.7	−57.3

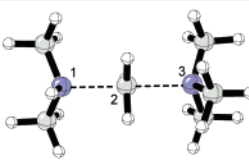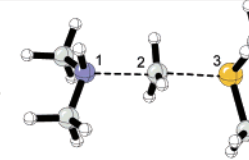mental activation free energies is found to be 1.9 kcal/mol with the UA0 cavity model.
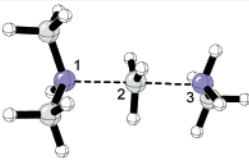
The sum of the gas-phase activation free energies obtained at the B3LYP/6-31+G(d,p) level of theory and solvation free energies computed with different cavity methods at the same level are given in Table 6. These values constitute estimates of the condensed-phase activation free energies and, therefore, are compared to the experimental values to assess the accuracy of the $\Delta\Delta G_{Sol}^{\ddagger}$'s obtained with different cavity models. The condensed-phase activation free energy for reaction C seems to be correlated better with the experimental value when the solvation corrections are computed with the UFF, BONDI, and PAULING cavity models, but the agreement between the experimental and computed values gets worse in the case of reactions A and B with these cavity models. The activation free energies with the BONDI and PAULING cavity models are systematically higher than the corresponding reactions with the UA0 cavity model (~7 kcal/mol). The average absolute errors for the computed activation free energies are 2.3 and 3.2 kcal/mol with the UFF and UA0 cavity models, respectively. The UFF cavity model appears to generate more reliable solvation free energies for the methyl-transfer reactions even though this cavity method was shown to produce larger deviations from experimental hydration energies in a more general benchmark.[39]

Aqueous-phase activation free energies for the methyl-transfer reactions computed by correcting the gas-phase CBS-QB3 activation free energies with GB/SA solvation corrections are given in Table 7. In order to obtain the solvation free energies for the DFT gas-phase geometries, the charges

for the DFT structures have been computed with the CM1 charge method by making use of the AM1[30] semiempirical Hamiltonian. After this step, CM1A charges were used to calculate the solvation free energies for the reactants, products, and transition structures with the GB/SA solvation method (Table 8). The average absolute error is found to be 5.4 kcal/mol with the GB/SA solvation corrections for the estimation of the activation free energies.

QM/MM/MC is another well-established method for the calculation of $\Delta G_{Sol}^{\ddagger}$ for chemical reactions. The QM/MM/MC explicit solvation method is a robust way of calculating accurate solvation free energies with explicit solute−solvent interactions.[32]

To permit a detailed elucidation of the changes in aqueous solvation along the reaction path, the QM/MM/MC treatment was used with the computation of free-energy profiles using FEP theory. The QM calculations were performed during the MC/FEP calculations using PDDG/PM3, and the solute geometries were fully sampled (see Methodology). The B3LYP/6-31+G(d,p) and PDDG/PM3 computed gas-phase transition structures of the three methyl-transfer reactions were very similar to the ones found by MC/FEP calculations (Figure 3). Radial distribution functions obtained between the carbon of the methyl group being transferred during the reaction (carbon 2 in Figure 3) and the oxygen of the surrounding water molecules at the TSs are shown in Figure 4. The PDDG/PM3 gas-phase activation enthalpies 31.3, 36.6, and 26.8 kcal/mol for reactions A, B, and C, respectively, differed notably from CBS-QB3 values despite the similarities between the predicted TSs (Table 1). Smooth free-energy profiles of the aqueous-phase reactions using a 0.01 Å increment predicted free energies of activation of 49.2, 50.1, and 39.3 kcal/mol from the PDDG/PM3/MM/MC simulations with cratic entropy corrections.[40] Even though PDDG/PM3/MM/MC simulations did not reproduce experimental activation free energies, the experimental trend was reproduced with these simulations.

Method	Transition state geometries and distances (Å) for reactions		
	A	B	C

	d(1-2)/d(2-3)	d(1-2)/d(2-3)	d(1-2)/d(2-3)
DFT	2.07 / 2.00	2.01 / 2.05	2.16 / 2.30
PDDG/PM3(gas)	1.98 / 1.96	2.00 / 2.01	2.00 / 2.24
PDDG/PM3(MC)	1.95 / 1.99	2.01 / 2.03	2.03 / 2.23

Figure 3. Geometrical comparison between gas-phase B3LYP/6-31+G(d,p) and PDDG/PM3 optimized transition state geometries in the gas phase and with the QM/MM/MC simulations. The structures from left to right are transition structure geometries for reactions A, B, and C.

Gunaydin et al.
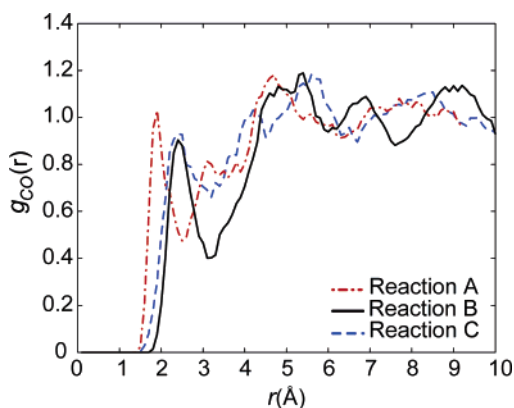
Figure 4. Radial distribution functions obtained from QM/MM/MC simulations for CBS-QB3 transition structures for reactions A, B, and C. *r* corresponds to the distance from carbon of the transferring methyl group to the water oxygens at the transition structures.

Conclusions

Activation enthalpies of the methyl-transfer reactions in the gas phase can be computed with reasonable accuracy with the B3LYP/6-31G(d,p) and MP2/6-31+G(d,p) levels of theory. Diffuse functions are found to be important in order to estimate the activation enthalpies accurately in the gas phase. Correcting the gas-phase CBS-QB3 free energies with the aqueous phase solvation free-energy corrections from CPCM calculations gave the free energy of activation with an average error of 1.9 kcal/mol. The PDDG/PM3 method overestimated the aqueous-phase activation free energies, but the qualitative trend was estimated correctly by this method.

Note Added after ASAP Publication. This article was released ASAP on March 10, 2007 with minor errors throughout the paper. The correct version was posted on March 19, 2007.

Supporting Information Available: Coordinates for all of the B3LYP/6-31+G**, MP2/6-31+G**, CBS-QB3, and PDDG/PM3 optimized structures. This material is available free of charge via teh Internet at http://pubs.acs.org.

References

(1) Shields, D. J.; Altarejos, J. Y.; Wang, X.; Agellon, L. B.; Vance, D. E. *J. Biol. Chem.* **2003**, *278*, 35826−35836.

(2) Zubieta, C.; Kota, P.; Ferrer, J-L.; Dixon, R. A.; Noel, J. P. *Plant Cell* **2002**, *14*, 1265−1277.

(3) Akashi, T.; Sawada, Y.; Shimada, N.; Sakurai, N.; Aoki, T.; Ayabe, S. *Plant Cell Physiol.* **2003**, *44*, 103−112.

(4) Lavid, N.; Schwab, W.; Kafkas, E.; Kock-Dean, M.; Bar, E.; Larkov, O.; Ravid, U.; Lewinsohn, E. *J. Agric. Food Chem.* **2002**, *50*, 4025−4030.

(5) Pancheri, P.; Scapicchio, P.; Chiaie, R. D. *Am. J. Clin. Nutr.* **2002**, *76*, 1158S−61S.

(6) Wang, L.; Thomae, B.; Eckloff, B.; Wieben, E.; Weinshilboum, R. *Biochem. Pharmacol.* **2002**, *64*, 699−710.

(7) Osipiuk, J.; Walsh, M. A.; Joachimiak, A. *Nucleic Acids Res.* **2003**, *31*, 5440−5448.

(8) Chen, L.; MacMillan, A. M.; Chang, W.; Ezaz-Nikpay, K.; Lane, W. S.; Verdine, G. L. *Biochemistry* **1991**, *30*, 11018−11025.

(9) Schluckebier, G.; O'Gara, M., Saenger, W.; Cheng, X. *J. Mol. Biol.* **1995**, *247*, 16−20.

(10) Callahan, B. P.; Wolfenden, R. *J. Am. Chem. Soc.* **2003**, *125*, 310−311.

(11) (a) Warshel, A.; Weiss, R. M. *J. Am. Chem. Soc.* **1980**, *102*, 6218−6226. (b) Warshel A. *Proc. Natl. Acad. Sci. U.S.A.* **1978**, *75*, 5250−5254. (c) Florian, J.; Warshel, A. *J. Phys. Chem. B* **1998**, *102*, 719−734. (d) Strajbl, M.; Florian, L.; Warshel, A. *J. Am. Chem. Soc.* **2000**, *122*, 5354−5366.

(12) (a) Roca, M.; Marti, S.; Andres, J.; Moliner, V.; Tunon, I.; Bertran, J.; Williams, I. H. *J. Am. Chem. Soc.* **2003**, *125,* 7726−7737. (b) Kuhn, B.; Kollman, P. A. *J. Am. Chem. Soc.* **2000**, *122,* 2586−2596. (c) Zheng, Y.-J.; Bruice, T. C. *J. Am. Chem. Soc.* **1997**, *119,* 8137. (d) Lau, E. Y.; Bruice, T. C. *J. Am. Chem. Soc.* **2000**, *122,* 7165−7171. (e) Kahn, K.; Bruice, T. C. *J. Am. Chem. Soc.* **2000**, *122*, 46−51.

(13) Castejon, H.; Wiberg, K. B.; Sklenak, S.; Hinz, W. *J. Am. Chem. Soc.* **2001**, *123*, 6092−6097.

(14) Vayner, G.; Houk, K. N.; Jorgensen, W. L.; Brauman, J. I. *J. Am. Chem. Soc.* **2004**, *126*, 9054−9058.

(15) Parr, R. G.; Yang, W. *Density Functional Theory of Atoms and Molecules*; Oxford University Press: New York, 1989.

(16) Handy, N. C. Density Functional Theory, In *Lecture Notes in Quantum Chemistry*; Roos, B. O., Ed.; Springer-Verlag: Berlin, 1994; Vol. 2, pp 91−123.

(17) Møller, C.; Plesset, M. S. *Phys. Rev.* **1934**, *46*, 618−622.

(18) Montgomery, J. A., Jr.; Frisch, M. J.; Ochterski, J. W.; Petersson, G. A. *J. Chem. Phys.* **1999**, *110*, 2822−2827.

(19) Frisch, M. J.; Trucks, G. W.; Schlegel, H. B.; Scuseria, G. E.; Robb, M. A.; Cheeseman, J. R.; Zakrzewski, V. G.; Montgomery, J. A., Jr.; Stratmann, R. E.; Burant, J. C.; Dapprich, S.; Millam, J. M.; Daniels, A. D.; Kudin, K. N.; Strain, M. C.; Farkas, O.; Tomasi, J.; Barone, V.; Cossi, M.; Cammi, R.; Mennucci, B.; Pomelli, C.; Adamo, C.; Clifford, S.; Ochterski, J.; Petersson, G. A.; Ayala, P. Y.; Cui, Q.; Morokuma, K.; Malick, D. K.; Rabuck, A. D.; Raghavachari, K.; Foresman, J. B.; Cioslowski, J.; Ortiz, J. V.; Stefanov, B. B.; Liu, G.; Liashenko, A.; Piskorz, P.; Komaromi, I.; Gomperts, R.; Martin, R. L.; Fox, D. J.; Keith, T.; Al-Laham, M. A.; Peng, C. Y.; Nanayakkara, A.; Gonzalez, C.; Challacombe, M.; Gill, P. M. W.; Johnson, B. G.; Chen, W.; Wong, M. W.; Andres, J. L.; Head-Gordon, M.; Replogle, E. S.; Pople, J. A. *Gaussian 98*, revision A.5; Gaussian, Inc.: Pittsburgh, PA, 1998.

(20) Frisch, M. J.; Trucks, G. W.; Schlegel, H. B.; Scuseria, G. E.; Robb, M. A.; Cheeseman, J. R.; Montgomery, J. A., Jr.; Vreven, T.; Kudin, K. N.; Burant, J. C.; Millam, J. M.; Iyengar, S. S.; Tomasi, J.; Barone, V.; Mennucci, B.; Cossi, M.; Scalmani, G.; Rega, N.; Petersson, G. A.; Nakatsuji, H.; Hada, M.; Ehara, M.; Toyota, K.; Fukuda, R.; Hasegawa, J.; Ishida, M.; Nakajima, T.; Honda, Y.; Kitao, O.; Nakai, H.; Klene, M.; Li, X.; Knox, J. E.; Hratchian, H. P.; Cross, J. B.; Bakken, V.; Adamo, C.; Jaramillo, J.; Gomperts, R.; Stratmann, R. E.; Yazyev, O.; Austin, A. J.; Cammi, R.;

Pomelli, C.; Ochterski, J. W.; Ayala, P. Y.; Morokuma, K.; Voth, G. A.; Salvador, P.; Dannenberg, J. J.; Zakrzewski, V. G.; Dapprich, S.; Daniels, A. D.; Strain, M. C.; Farkas, O.; Malick, D. K.; Rabuck, A. D.; Raghavachari, K.; Foresman, J. B.; Ortiz, J. V.; Cui, Q.; Baboul, A. G.; Clifford, S.; Cioslowski, J.; Stefanov, B. B.; Liu, G.; Liashenko, A.; Piskorz, P.; Komaromi, I.; Martin, R. L.; Fox, D. J.; Keith, T.; Al-Laham, M. A.; Peng, C. Y.; Nanayakkara, A.; Challacombe, M.; Gill, P. M. W.; Johnson, B.; Chen, W.; Wong, M. W.; Gonzalez, C.; Pople, J. A. *Gaussian 03*, revision C.02; Gaussian, Inc.: Wallingford, CT, 2004.

(21) Becke, A. D. *J. Chem. Phys.* **1993**, *98*, 5648−5652.

(22) Lee, C.; Yang, W.; Parr, R. G. *Phys. Rev. B: Condens. Matter Mater. Phys.* **1988**, *37*, 785−789.

(23) Lynch, B. J.; Fast, P. L.; Harris, M.; Truhlar, D. G. *J. Phys. Chem. A* **2000**, *104*, 4811−4815.

(24) Barone, V.; Cossi, M. *J. Phys. Chem. A* **1998**, *102*, 1995−2001.

(25) Hasel, W.; Hendrickson, T. L.; Still, W. C. *Tetrahedron Comput. Methodol.* **1988**, *1*, 103−116.

(26) Jorgensen, W. L.; Ulmschneider, J. P.; Tirado-Rives, J. *J. Phys. Chem. B* **2004**, *108*, 16264−16270.

(27) Udier-Blagociv, M.; De Tirano, P. M.; Pearlman, S. A.; Jorgensen, W. L. *J. Comput. Chem.* **2004**, *25*, 1322−1332.

(28) Jorgensen, W. L.; Tirado-Rives, J. *J. Comput. Chem.* **2005**, *26*, 1689−1700.

(29) Storer, J. W.; Giesen, D. J.; Cramer, C. J.; Truhlar, D. G. *J. Comput.-Aided Mol. Des.* **1995**, *9*, 87−110.

(30) Dewar, M. J. S.; Zoebisch, E. G.; Healy, E. F.; Stewart, J. J. P. *J. Am. Chem. Soc.* **1985**, *107*, 3902−3909.

(31) (a) Gogonea, V. *Internet Electron. J. Mol. Des.* **2002**, *1*, 173−184. (b) Warshel A.; Levitt M. *J. Mol. Biol.* **1976**, *103*, 227−249. (c) Singh, U. C.; Kollman, P. A. *J. Comput. Chem.* **1986**, *7*, 718−730. (d) Field, M. J.; Bash, P. A.; Karplus, M. *J. Comput. Chem.* **1990**, *11*, 700−733. (e) Maseras, F.; Morokuma, K. *J. Comput. Chem.* **1995**, *16*, 1170−1179. (f) Guimaraes, C. R. W.; Udier-Blagovic, M.; Jorgensen, W. L. *J. Am. Chem. Soc.* **2005**, *127*, 3577−3588. (g) Guimaraes, C. R. W.; Repasky, M. P.; Chandrasekhar, J.; Tirado-Rives, J.; Jorgensen, W. L. *J. Am. Chem. Soc.* **2003**, *125*, 6892−6899.

(32) (a) Acevedo, O.; Jorgensen, W. L. *Org. Lett.* **2004**, *6*, 2881−2884. (b) Acevedo, O.; Jorgensen, W. L. *J. Am. Chem. Soc.* **2005**, *127*, 8829−8834. (c) Acevedo, O.; Jorgensen, W. L. *J. Org. Chem.* **2006**, *71*, 4896−4902. (d) Acevedo, O.; Jorgensen, W. L. *J. Am. Chem. Soc.* **2006**, *128*, 6141−6144.

(33) (a) Repasky, M. P.; Chandrasekhar, J.; Jorgensen, W. L. *J. Comput. Chem.* **2002**, *23*, 1601−1622. (b) Tubert-Brohman, I.; Guimaraes, C. R. W.; Repasky, M. P.; Jorgensen, W. L. *J. Comput. Chem.* **2003**, *25*, 138−150. (c) Tubert-Brohman, I.; Guimaraes, C. R. W.; Jorgensen, W. L. *J. Chem. Theory Comput.* **2005**, *1*, 817−823.

(34) Jorgensen, W. L.; Chandrasekhar, J.; Madura, J. D.; Impey, W.; Klein, M. L. *J. Chem. Phys.* **1983**, *79*, 926−935.

(35) Glukhovtsev, M. N.; Bach, R. D.; Pross, A.; Radom, L. *Chem. Phys. Lett.* **1996**, *260*, 558−564.

(36) Martin, J. M. L.; De Oliveria, G. *J. Chem. Phys.* **1991**, *111*, 1843−1856.

(37) Parthiban, S.; De Oliveria, G.; Martin, J. M. L. L. *Phys. Chem. A* **2001**, *105*, 895−904.

(38) Botchwina, P. *Theor. Chem. Acc.* **1998**, *99*, 426−428.

(39) Takano, Y.; Houk, K. N. *J. Chem. Theory Comput.* **2005**, *1*, 70−77.

(40) Yu, B. Y. *J. Pharm. Sci.* **2001**, *90*, 2099−2102.